Coordinatively unsaturated cobalt ion in Co^+ (H_20)n (n = 4-6) probed with infrared photodissociation spectroscopy

Furukawa, Kazuki
Department of Chemistry, Graduate School of Sciences, Kyushu University

Ohashi, Kazuhiko
Department of Chemistry, Faculty of Sciences, Kyushu University

Koga, Nobuhiro
Department of Chemistry, Graduate School of Sciences, Kyushu University

Imamura, Toshitaka
Department of Chemistry, Graduate School of Sciences, Kyushu University

他

https://hdl.handle.net/2324/25476

KYUSHU UNIVERSITY

Coordinatively unsaturated cobalt ion in $Co^+(H_2O)_n$ ($n = 4–6$) probed with infrared photodissociation spectroscopy

Kazuki Furukawa [a], Kazuhiko Ohashi [b,*], Nobuhiro Koga [a], Toshitaka Imamura [a], Ken Judai [c], Nobuyuki Nishi [c], Hiroshi Sekiya [b]

[a] *Department of Chemistry, Graduate School of Sciences, Kyushu University,*

Hakozaki, Fukuoka 812-8581, Japan

[b] *Department of Chemistry, Faculty of Sciences, Kyushu University,*

Hakozaki, Fukuoka 812-8581, Japan

[c] *Institute for Molecular Science, Myodaiji, Okazaki 444-8585, Japan*

Abstract

The hydrated cobalt ions, $Co^+(H_2O)_n$ ($n = 4–6$), are studied with the infrared (IR) photodissociation spectroscopy in the OH-stretch region and density functional theory calculations.   The calculations predict a T-shaped coordination structure for $Co^+(H_2O)_3$, which exposes empty coordination sites for additional H_2O ligands.   Nevertheless, the IR spectrum of $Co^+(H_2O)_4$ indicates that the fourth H_2O prefers to occupy the second shell through H-bonding rather than coordinate directly to Co^+.   A comparison between the experimental and theoretical IR spectra suggests that the T-shaped coordination remains intact in the $n = 4–6$ ions, leaving the direct coordination sites unoccupied.

---

[*] Corresponding author.   Fax: +81-92-642-2607.

1. Introduction

Hydrated metal ions have been the subject of extensive theoretical and experimental research, because such species play important roles in many chemical and biological systems. Studies of hydrated metal ions in the gas phase have provided powerful ways to understand the intermolecular interactions commonly found in condensed phases [1].   Cobalt is an essential element for life, as it is a key constituent of vitamin B_{12} [2].   An ordinary oxidation state for simple compounds of cobalt is +2; Co(II) salts form the red-pink $[Co(H_2O)_6]^{2+}$ complex in aqueous solutions [3].   Although Co(I) is unstable in aqueous solutions, the $Co^+(H_2O)_n$ ions have attracted attention in a number of gas-phase experiments [4–8] and theoretical calculations [9–16].   The stepwise binding energies of $Co^+(H_2O)_n$ ($n = 1$–4) were measured through collision-induced dissociation (CID) experiments [4–8].   The electronic states of $Co^+(H_2O)_n$ ($n = 1$–10) were probed with photofragmentation experiments [8]. Various computational methods were applied for predicting structures, binding energies, and vibrational frequencies of $Co^+(H_2O)_1$ and $Co^+(H_2O)_2$ [9–16].

For transition-metal ions, metal–ligand bonding is expected to be more than simple electrostatic interactions [9,10].   The electronic configurations of Co^+ and Ni^+ in the ground state are $(3d)^8$ and $(3d)^9$, respectively.   These configurations result in non-spherical distributions of the total electron density, which may lead to a coordination structure specific to each metal ion.   Mass spectra of Co^+ and Ni^+ solvated by Ar atoms showed anomalously strong peaks at $n = 6$ for Co^+Ar_n [17] and $n = 4$ for Ni^+Ar_n [18].   For explaining these magic numbers, a simple model was proposed [18,19], which predicts an octahedral coordination for Co^+Ar_6 and a square-planar coordination for Ni^+Ar_4.   Concerning hydration, infrared (IR) spectroscopy revealed that $Ni^+(H_2O)_n$ prefers a coordination number of 4 [20], which is consistent with the square-planar coordination predicted for Ni^+.   On the other hand, a coordination number of 6 is expected for $Co^+(H_2O)_n$ from the octahedral coordination predicted for Co^+.   However, Poisson et al. [8] reported the preference for smaller coordination numbers of $Co^+(H_2O)_n$: 3 for $n = 4$ and 5; ≥ 4 for $n = 9$ and 10.

We have applied the IR photodissociation spectroscopy [20–22] to $Co^+(H_2O)_n$ in the

present work for establishing the coordination number of Co^+ in these ions.   Complementary theoretical calculations have been carried out for predicting minimum-energy structures and corresponding IR spectra of $Co^+(H_2O)_n$.   We have found evidence that H_2O molecules start to occupy the second shell, even though the first shell is not closed seemingly.

2. Experimental and computational methods

The IR photodissociation spectra were measured by using a triple quadrupole mass spectrometer [23].   The $Co^+(H_2O)_n$ ions were produced by laser vaporization of a cobalt rod in a supersonic expansion of H_2O in Ar.   The parent ions of interest were isolated by the first quadrupole mass filter.   In the second quadrupole ion guide, the ions were irradiated with the output of an IR optical parametric oscillator (OPO) system (Continuum, Mirage 3000).   The resulting fragment ions were analyzed by the third quadrupole mass spectrometer.   The spectra of $Co^+(H_2O)_n$ were obtained by recording the yields of the $Co^+(H_2O)_{n-1}$ fragment ions as a function of IR wavenumber.

Theoretical calculations were carried out with the GAUSSIAN 03 program package [24]. Density functional theory (DFT) method was employed with the B3LYP functional and the 6-311+G(2df) and 6-31+G(d) basis sets for cobalt and other atoms, respectively.   Stable structures, vibrational frequencies, and IR absorption intensities were calculated for $Co^+(H_2O)_n$. The harmonic frequencies were scaled with a factor of 0.976, which was chosen to reproduce the average of the symmetric (3657 cm^{-1}) and antisymmetric (3756 cm^{-1}) OH-stretching frequencies of the gas-phase H_2O molecule [25].

3. Results and discussion

3.1. Minimum-energy structures

Theoretical calculations were already carried out for $Co^+(H_2O)_1$ [9–16] and $Co^+(H_2O)_2$ [9,10].   These studies indicated that an H_2O molecule binds to the Co^+ ion via the oxygen atom, forming the $Co^+(H_2O)_1$ complex with a C_{2v} structure.   Two H_2O molecules bind opposite each other in $Co^+(H_2O)_2$, resulting in a twofold linear coordination.   The results of our DFT

calculations are consistent with those of the previous ones.

Fig. 1a displays the lowest-energy structure of $Co^+(H_2O)_3$ obtained from our DFT calculations. Three H_2O molecules bind to Co^+ in a T-shaped arrangement. The Co^+–O bond of the stem H_2O (2.20 Å) is longer than those of the top molecules (1.97 Å) and the angle between the shorter bonds is 170°. Fig. 1b–e shows minimum-energy structures of $Co^+(H_2O)_4$. The labeling ($l+m$) is used to classify the solvation structures, where l stands for the coordination number, m is the number of molecules in the second solvation shell, and subscripts are added to m for specifying H-bonding sites, when necessary. Four H_2O molecules in (4+0) (Fig. 1b) adopt a slightly distorted square-planar coordination. The Co^+–O bonds of the vertical ligands (2.24 Å) are longer than those of the horizontal ligands (2.02 Å). Meanwhile, the T-shaped coordination remains intact in all (3+1) isomers, placing one H_2O in the second shell. It is H-bonded to the stem H_2O in $(3+1_s)$ (Fig. 1c) or to a top H_2O in $(3+1_t)$ (Fig. 1d), both in a single acceptor configuration. The external H_2O in $(3+1_b)$ (Fig. 1e) bridges two first-shell molecules in a double acceptor H-bonding configuration. The DFT calculations predict that $(3+1_b)$ is the most stable structure; $(3+1_t)$, (4+0), and $(3+1_s)$ are higher in energy than $(3+1_b)$ by 4, 7, and 14 kJ mol^{-1}, respectively.

3.2. IR spectra

Because the photodissociation yield was very small for $Co^+(H_2O)_n$ with $n = 1–3$, it was necessary to employ a tagging technique [26,27] to measure the IR spectra. Details of the results will be published separately [28], but it is worth noting here that the IR spectra for $n = 1–3$ are consistent with coordination structures in which all H_2O molecules bind to Co^+ directly.

For $n \geq 4$, we were able to measure the spectra of $Co^+(H_2O)_n$ without tagging. In Fig. 2, the experimental spectrum of $Co^+(H_2O)_4$ is compared with the theoretical spectra for the isomers presented in Fig. 1b–e. All theoretical spectra display transitions due to free-OH groups in the 3600–3750 cm^{-1} region. In addition, three (3+1) isomers exhibit transitions characteristic of H-bonded-OH groups in lower frequency region. The H-donating H_2O in

$(3+1_t)$ is expected to be polarized by the metal charge more significantly than that in $(3+1_s)$, because the Co^+–O distance concerned is 1.94 Å for $(3+1_t)$ and 2.15 Å for $(3+1_s)$.   As a result, the H-bond in $(3+1_t)$ is stronger than that in $(3+1_s)$; the H-bonded-OH transition of $(3+1_t)$ (3191 cm^{-1}) is lower in frequency than that of $(3+1_s)$ (3325 cm^{-1}).   Both these frequencies are lower than those of $(3+1_b)$ (3406 and 3513 cm^{-1}), because the linear H-bonds in $(3+1_t)$ and $(3+1_s)$ are stronger than the bent H-bonds in $(3+1_b)$.   The experimental spectrum (Fig. 2a) shows unresolved features in the free-OH region.   In addition, two broad maxima are observed around 3160 and 3315 cm^{-1}, which are assignable to the 3191 cm^{-1} transition of $(3+1_t)$ and the 3325 cm^{-1} transition of $(3+1_s)$, respectively.   The experimental spectrum can be reproduced by a superposition of the theoretical spectra for $(3+1_t)$ and $(3+1_s)$. This implies that significant part of the fourth H_2O molecules prefer the H-bonding sites in the second shell rather than the direct coordination site.

Our previous study [29] revealed that the coordination number of $Ag^+(H_2O)_3$ varies depending on the temperature of the ion; a 3-coordinated structure is dominant under cold conditions achieved with Ar-tagging, although a 2-coordinated isomer is dominant under warm conditions without tagging.   In light of these results, we applied the tagging technique to $Co^+(H_2O)_4$; we used N_2 instead of Ar as a tag, because the amount of the Ar-tagged ions prepared in our ion source was not large enough for the IR spectroscopic study.   Fig. 2f shows the IR photodissociation spectrum of $Co^+(H_2O)_4 \cdot N_2$.   The spectrum exhibits four distinct bands at 3430, 3520, 3620, and 3700 cm^{-1}.   The 3430 and 3520 cm^{-1} bands correspond to the 3406 and 3513 cm^{-1} transitions of $(3+1_b)$, respectively, which are due to the OH groups involved in the bent H-bonds.   The overall features are in excellent agreement with the theoretical spectrum of $(3+1_b)$, indicating that $(3+1_b)$ is the predominant structure. If $(4+0)$ would be predominant, the observed free-OH bands would be much stronger than the H-bonded-OH bands.   The predominance of the $(3+1_b)$ structure under cold conditions is consistent with the theoretical prediction that it is the most stable isomer of $Co^+(H_2O)_4$.

In order to probe the binding sites for additional H_2O molecules, we measured the IR spectra of $Co^+(H_2O)_5$ and $Co^+(H_2O)_6$.   Unfortunately, we were not able to produce an enough

amount of the N_2-tagged ions.   Shown in Fig. 3b–e are the optimized structures and theoretical IR spectra for two (3+2) and two (4+1) isomers of $Co^+(H_2O)_5$.   Both (3+2) structures retain the T-shaped coordination.   Two second-shell molecules are separately H-bonded to a top H_2O and the stem H_2O in (3+2$_{ts}$), whereas to different top molecules in (3+2$_{tt}$).   The H-bonded-OH transitions are located at 3235 and 3344 cm^{-1} for (3+2$_{ts}$), while at 3238 and 3277 cm^{-1} for (3+2$_{tt}$).   On the other hand, both (4+1) structures adopt the square-planar coordination.   The second-shell H_2O in (4+1$_d$) is a dangling single acceptor secured by one first-shell molecule, whereas it bridges two first-shell molecules in (4+1$_b$). The H-bonded-OH transition is located at 3335 cm^{-1} for (4+1$_d$), while at 3459 and 3517 cm^{-1} for (4+1$_b$).   The experimental spectrum (Fig. 3a) shows strong absorption with a maximum around 3225 cm^{-1} and a tail in the 3300–3500 cm^{-1} region.   Although the positions of the H-bonded-OH transitions of the (4+1) isomers are consistent with the high-frequency tail, there is no transition corresponding to the 3225 cm^{-1} maximum.   Thus the (4+1) isomers alone are not enough to explain the experimental spectrum.   The 3225 cm^{-1} maximum is most likely to originate from the 3235 cm^{-1} transition of (3+2$_{ts}$) or 3238 cm^{-1} transition of (3+2$_{tt}$), or both.   Accordingly, the presence of at least one (3+2) structure is necessary to reproduce the overall features of the experimental spectrum.

Fig. 4 compares the experimental IR spectrum of $Co^+(H_2O)_6$ with the theoretical spectra for two (3+3) and two (4+2) isomers.   Both (3+3) structures retain the T-shaped coordination, while both (4+2) structures adopt the square-planar coordination.   As in the case of $n = 5$, the presence of at least one (3+3) structure is necessary to reproduce the experimental spectrum, particularly the multiple bands observed in the 3100–3400 cm^{-1} region.

As discussed previously [30], the internal energy content of the ions prepared in our source may be close to that of the evaporative ensemble [31].   In such a case, the temperature of the ions is parametrically dependent on the binding energy; the ions with smaller binding energies have lower temperatures.   Although no experimental data are available for $n \geq 5$, the binding energies of $Co^+(H_2O)_n$ should decrease with increasing n, and so do the temperatures.

For larger n, accordingly, we expect less pronounced differences between the IR spectra measured with and without tagging.   The IR spectra recorded for $Co^+(H_2O)_5$ and $Co^+(H_2O)_6$ suggest that significant part of the fifth and sixth H_2O molecules also prefer the H-bonding sites in the second shell, leaving the fourth coordination site of Co^+ unoccupied.   The coordination of the Co^+ ion in $Co^+(H_2O)_n$ ($n = 4$–6) is unsaturated seemingly.

3.3. Coordinative unsaturation

Let us first review the coordination structure of Ni^+ for a comparison purpose.   In a mass spectrum of Ni^+Ar_n, Velegrakis et al. [18] found an anomalously large abundance of the n = 4 ion.   In order to account for the anomalous stability of Ni^+Ar_4, they used what we call 'orbital orientation model', which was proposed by Beyer et al. [19].   The crucial point is the assumption that the Ar ligands seek out electron-density minima in the valence shell of the metal ion [18,19].   The ground state of Ni^+ is ^2D with a $(3d)^9$ configuration; there are four fully-filled and one half-filled 3d orbital.   If the latter is identified with the $3d(x^2$–$y^2)$ orbital, it provides four electron-density minima along the x and y axes.   This results in a strong interaction with only four Ar atoms, and thus, a square-planar complex.   In support of this model, the DFT calculations revealed the square-planar coordination for Ni^+Ar_4 [18].   As for hydration of Ni^+, Walters et al. [20] reported the IR photodissociation spectra of $Ni^+(H_2O)_n$. They showed that the spectrum of $Ni^+(H_2O)_4$ is consistent with a (4+0) structure, although a minor (3+1) isomer is present.   Thus, this model is successful in explaining the coordination number and structure of $Ni^+(H_2O)_n$ as well as Ni^+Ar_n.

In a mass spectrum of Co^+Ar_n, Lessen and Brucat [17] found a magic number at $n = 6$. The ground state of Co^+ is ^3F with a $(3d)^8$ configuration; there are three fully-filled and two half-filled 3d orbitals.   If the latter are identified with the $3d(x^2$–$y^2)$ and $3d(z^2)$ orbitals, they provide six electron-density minima along the x, y, and z axes.   This results in the coordination of six Ar atoms, and thus, an octahedral Co^+Ar_6 complex.   One might expect the same coordination structure for $Co^+(H_2O)_6$, because isoelectronic species, $[Ni^{II}(H_2O)_6]^{2+}$ and $[Cu^{III}(H_2O)_6]^{3+}$, also favor the octahedral coordination [3].   However, Poisson et al. [8]

reported the preference for smaller coordination numbers.   In particular, they suggested that both $Co^+(H_2O)_4$ and $Co^+(H_2O)_5$ take 3-coordinated structures exclusively.   Our IR spectroscopic results are consistent with this suggestion, because the experimental spectra of $Co^+(H_2O)_4$ and $Co^+(H_2O)_5$ can be reproduced by the 3-coordinated structures alone without including the 4-coordinated structures.

The T-shaped coordination of $Co^+(H_2O)_3$ is consistent with the orbital orientation model, because the occupation of three out of six electron-density minima of Co^+ results in such a coordination.   Nonetheless, the observation of the (3+1) and (3+2) structures with the T-shaped core is a surprise to us, because it seems that at least one coordination site of Co^+ remains empty.   Previously, our group [32,33] confirmed that solvent molecules occupy the second shell of Mg^+, even though the first shell is not closed apparently.   For Mg^+, however, it is obvious why the coordination is not saturated.   Because of a 3s electron localized in the vicinity of the metal, only a limited number of solvent molecules are allowed to occupy the first shell and additional molecules are not able to squeeze into the first shell.   One must recognize that the situation is completely different for the $Co^+(H_2O)_n$ system.   The Co^+ ion in $Co^+(H_2O)_3$ exposes empty coordination sites for additional ligands.   Actually, there is a potential-energy minimum corresponding to the (4+0) structure, as described in section 3.1. Moreover, the (4+0) minimum lies only 7 kJ mol^{-1} above the global $(3+1_b)$ minimum. Therefore, the predominant population of the (3+1) structures may be caused by a factor other than the energetics.   In our ion source of a laser-vaporization/supersonic expansion type, the hydrated ions are likely to grow by stepwise addition of H_2O molecules to Co^+; the $Co^+(H_2O)_4$ ions are formed by the association reaction of $Co^+(H_2O)_3$ with H_2O.   We constructed potential energy surfaces of this system for exploring the formation mechanism of $Co^+(H_2O)_4$. Fig. 5 displays a 2-dimensional surface calculated as functions of R and θ (see inset of Fig. 5 for definition); other geometrical parameters were fixed at the values of the (4+0) structure. A minimum located at $R \approx 2.24$ Å and $\theta \approx 100°$ corresponds to the (4+0) structure.   Deeper potential wells associated with the $(3+1_t)$ structures are not located on this surface, but such wells correlate with two minima at $R \approx 4.5$ Å and $\theta \approx 25°$ and at $R \approx 4.1$ Å and $\theta \approx 135°$.

Now we can picture the following scenario for the preferential formation of the (3+1) structures. The potential energy decreases monotonically with decreasing R toward the (4+0) minimum only when the trajectories come in at $\theta \approx 90°$. If the initial values of θ deviate from 90°, the incoming trajectories make a turn to one of the $(3+1_t)$ minima. Because there is a barrier (≈ 16 kJ mol^{-1} in height from the bottom of the true $(3+1_t)$ well) for isomerization from the $(3+1_t)$ to (4+0) structure, most part of the trajectories may be trapped in the $(3+1_t)$ wells. Although the relevant region is not shown in Fig. 5, one can easily imagine that the trajectories with $180° < \theta < 360°$ reach one of the minima corresponding to the $(3+1_b)$ and $(3+1_s)$ structures. Potential energy surfaces of higher dimensions calculated at higher levels of theory are required for discussing more quantitative aspects of the formation mechanism of $Co^+(H_2O)_4$.

The second shell of the T-shaped core is filled with six H_2O molecules, because three first-shell molecules donate six OH groups. In the resulting $Co^+(H_2O)_9$ ion, all potential wells responsible for the (3+6) structure are already occupied. As a result, there may be a greater chance for the next H_2O molecule to reach the direct coordination site to form the 4-coordinated structure. Indeed, Poisson et al. [8] suggested a coordination number of 4 (and larger) for $Co^+(H_2O)_{10}$. In order to verify this suggestion, theoretical calculations and the analysis of the IR spectra for $Co^+(H_2O)_n$ ($n = 7$–10) are under way [28].

4. Conclusions

We have studied the $Co^+(H_2O)_n$ ($n = 4$–6) ions by the infrared photodissociation spectroscopy in the OH-stretch region with the complementary DFT calculations. A T-shaped coordination structure calculated for $Co^+(H_2O)_3$ is consistent with the orbital orientation model [18,19], where the $3d(x^2-y^2)$ and $3d(z^2)$ orbitals of Co^+ are assumed to be half-filled. The model predicts that the Co^+ ion exposes six coordination sites for ligands, which is supported by the anomalous stability of the Co^+Ar_6 ion [17]. However, the present IR spectrum of $Co^+(H_2O)_4$ indicates that the fourth H_2O molecule prefers to occupy the second shell through H-bonding rather than coordinate directly to Co^+. Moreover, the IR

spectra of $Co^+(H_2O)_5$ and $Co^+(H_2O)_6$ can be reproduced by the 3-coordinated structures alone without including the 4-coordinated structures, suggesting that the direct coordination sites of the T-shaped core remain unoccupied.

In Co^+Ar_n, the Ar ligands have no choice but bind directly to Co^+ until the coordinative saturation at $n = 6$, because the Ar–Ar binding energy is considerably small.   In $Co^+(H_2O)_n$, however, the fourth and additional H_2O molecules possibly occupy the second shell through H-bonding, because such H-bonds can be substantially strong [7,8,34]. Actually, the DFT calculations predict that $(3+1_b)$ is the most stable structure of $Co^+(H_2O)_4$. Nevertheless, (4+0) is also a stable structure and is only 7 kJ mol^{-1} higher in energy than $(3+1_b)$.   Therefore, it is unlikely that the energetics of $Co^+(H_2O)_4$ is responsible for the preferential formation of the (3+1) structures.   A plausible explanation is made on the basis of the topology of the potential energy surface; the minima associated with the (3+1) structures trap the incoming fourth H_2O molecule and prevent the direct coordination to Co^+.

References

[1] M. Beyer, Mass Spectrom. Rev. 56 (2007) 517.

[2] S.J. Lippard, J.M. Berg, Principles of Bioinorganic Chemistry, University Science Books, Mill Valley, 1994.

[3] F.A. Cotton, G. Wilkinson, P.L. Gauss, Basic Inorganic Chemistry, Wiley, New York, 1995.

[4] T.F. Magnera, D.E. David, J. Michl, J. Am. Chem. Soc. 111 (1989) 4100.

[5] P.J. Marinelli, R.R. Squires, J. Am. Chem. Soc. 111 (1989) 4101.

[6] N.F. Dalleska, K. Honma, L.S. Sunderlin, P.B. Armentrout, J. Am. Chem. Soc. 116 (1994) 3519.

[7] L. Poisson, P. Pradel, F. Lepetit, F. Réau, J.-M. Mestdagh, J.-P. Visticot, Eur. Phys. J. D 14 (2001) 89.

[8] L. Poisson, L. Dukan, O. Sublemontier, F. Lepetit, F. Réau, P. Pradel, J.-M. Mestdagh, J.-P. Visticot, Int. J. Mass Spectrom. 220 (2002) 111.

[9] M. Rosi, C.W. Bauschlicher Jr., J. Chem. Phys. 90 (1989) 7264.

[10] M. Rosi, C.W. Bauschlicher Jr., J. Chem. Phys. 92 (1990) 1876.

[11] E. Magnusson, N.W. Moriarty, J. Comp. Chem. 14 (1993) 961.

[12] M. Trachtman, G.D. Markham, J.P. Glusker, P. George, C.W. Bock, Inorg. Chem. 37 (1998) 4421.

[13] A. Irigoras, O. Elizalde, I. Silanes, J.E. Fowler, J.M. Ugalde, J. Am. Chem. Soc. 122 (2000) 114.

[14] S.J. Klippenstein, C.-N. Yang, Int. J. Mass Spectrom. 201 (2000) 253.

[15] R.C. Dunbar, J. Phys. Chem. A. 106 (2002) 7328.

[16] Y. Nakao, K. Hirao, T. Taketsugu, J. Chem. Phys. 114 (2001) 5216.

[17] D. Lessen, P.J. Brucat, J. Chem. Phys. 91 (1989) 4522.

[18] M. Velegrakis, G.E. Froudakis, S.C. Farantos, J. Chem. Phys. 109 (1998) 4687.

[19] M. Beyer, C. Berg, G. Albert, U. Achatz, V.E. Bondybey, Chem. Phys. Lett. 280 (1997) 459.

[20] R.S. Walters, E.D. Pillai, M.A. Duncan, J. Am. Chem. Soc. 127 (2005) 16599.

[21] J.M. Lisy, Int. Rev. Phys. Chem. 16 (1997) 267.

[22] M.A. Duncan, Int. Rev. Phys. Chem. 22 (2003) 407.

[23] T. Iino, K. Ohashi, K. Inoue, K. Judai, N. Nishi, H. Sekiya, J. Chem. Phys. 126 (2007) 194302.

[24] M.J. Frisch et al., GAUSSIAN 03, Gaussian Inc., Wallingford CT, 2004.

[25] L.A. Pugh, K.N. Rao, J. Mol. Spectrosc. 47 (1973) 403.

[26] P. Ayotte, G.H. Weddle, J. Kim, M.A. Johnson, Chem. Phys. 239 (1998) 485.

[27] G. Gregoire, N.R. Brinkmann, D. van Heijnsbergen, H.F. Schaefer, M.A. Duncan, J. Phys. Chem. A 107 (2003) 218.

[28] K. Furukawa et al. (in preparation).

[29] T. Iino, K. Ohashi, K. Inoue, K. Judai, N. Nishi, H. Sekiya, Eur. Phys. J. D 43 (2007) 37.

[30] K. Inoue, K. Ohashi, T. Iino, K. Judai, N. Nishi, H. Sekiya, Phys. Chem. Chem. Phys. 9 (2007) 4793.

[31] C.E. Klots, Z. Phys. D, 5 (1987) 83.

[32] Y. Inokuchi, K. Ohshimo, F. Misaizu, N. Nishi, J. Phys. Chem. A 108 (2004) 5034.

[33] H. Machinaga, K. Ohashi, Y. Inokuchi, N. Nishi, H. Sekiya, Chem. Phys. Lett. 391 (2004) 85.

[34] A.J. Stace, Phys. Chem. Chem. Phys. 3 (2001) 1935.

Figure Captions

Fig. 1.   Structures of (a) (3+0) form of $Co^+(H_2O)_3$ and (b) (4+0), (c) $(3+1_s)$, (d) $(3+1_t)$, and (e) $(3+1_b)$ isomers of $Co^+(H_2O)_4$ optimized from DFT calculations.   Bond distances are in units of Å.

Fig. 2.   IR photodissociation spectra of (a) $Co^+(H_2O)_4$ and (f) $Co^+(H_2O)_4·N_2$.   Theoretical IR spectra of (b) (4+0), (c) $(3+1_s)$, (d) $(3+1_t)$, and (e) $(3+1_b)$ isomers of $Co^+(H_2O)_4$.

Fig. 3.   (a) IR photodissociation spectrum of $Co^+(H_2O)_5$.   Theoretical IR spectra and structures of (b) $(3+2_{ts})$, (c) $(3+2_{tt})$, (d) $(4+1_d)$, and (e) $(4+1_b)$ isomers of $Co^+(H_2O)_5$.

Fig. 4.   (a) IR photodissociation spectrum of $Co^+(H_2O)_6$.   Theoretical IR spectra and structures of (b) $(3+3_{tts})$, (c) $(3+3_{ttb})$, (d) $(4+2_{dd})$, and (e) $(4+2_{bb})$ isomers of $Co^+(H_2O)_6$.

Fig. 5.   Potential energy surface of the $Co^+(H_2O)_3 + H_2O$ system as functions of R and θ. Energies are in units of kJ mol^{-1}, relative to the value at $R = \infty$.   The surface is not symmetrical about the line of $\theta = 90°$, because the (4+0) structure is slightly distorted from a perfect square-planar geometry.
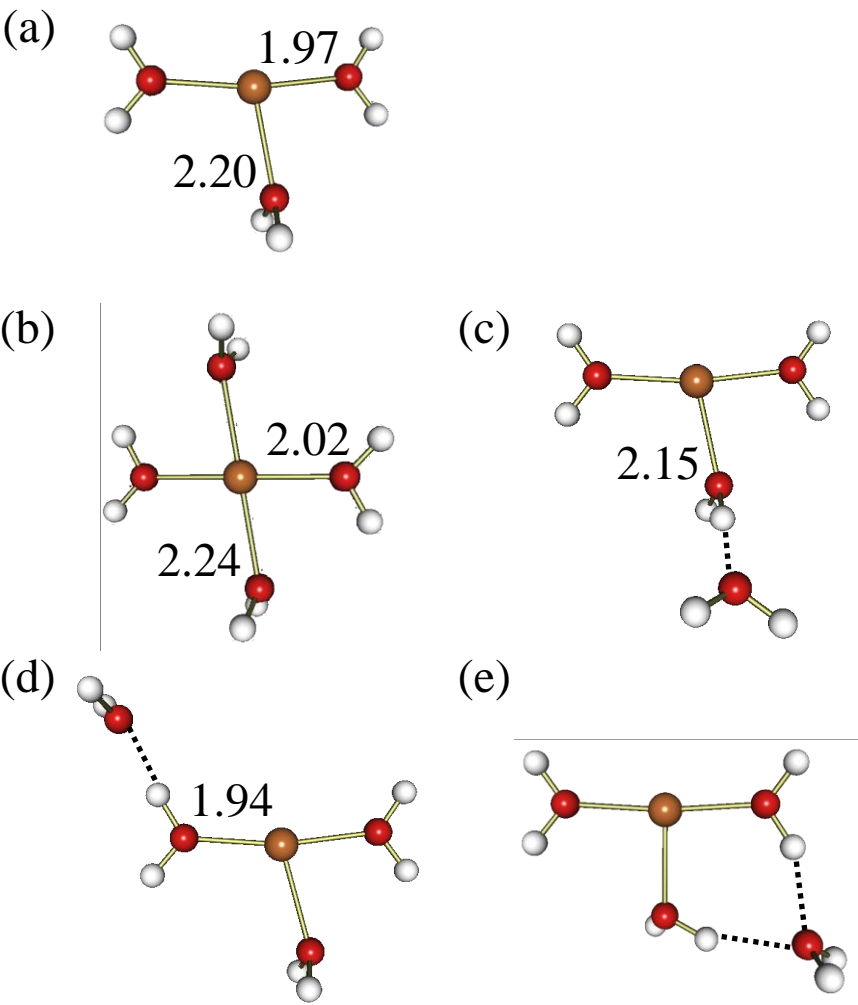
Figure 1

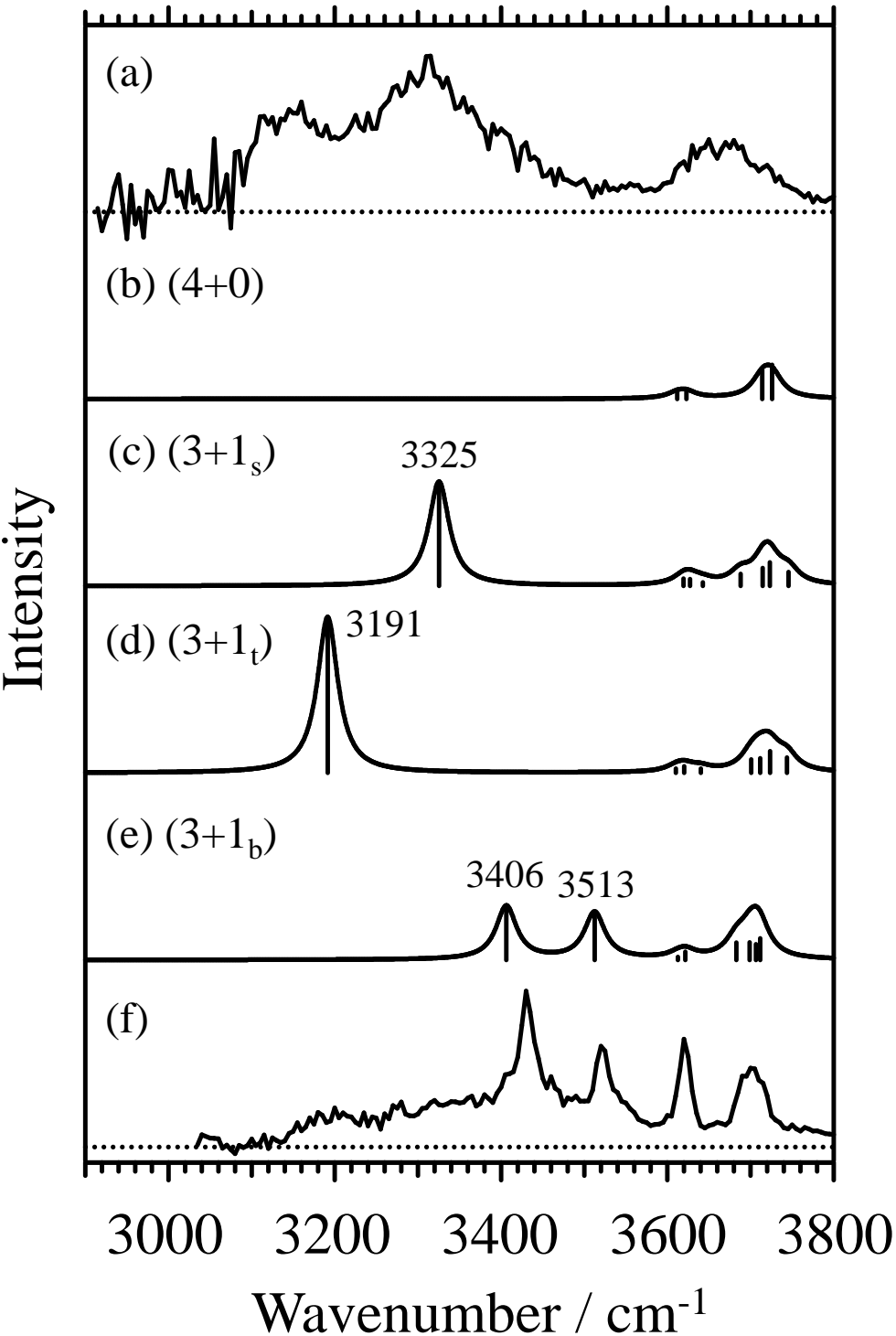(a) 1.97 2.20
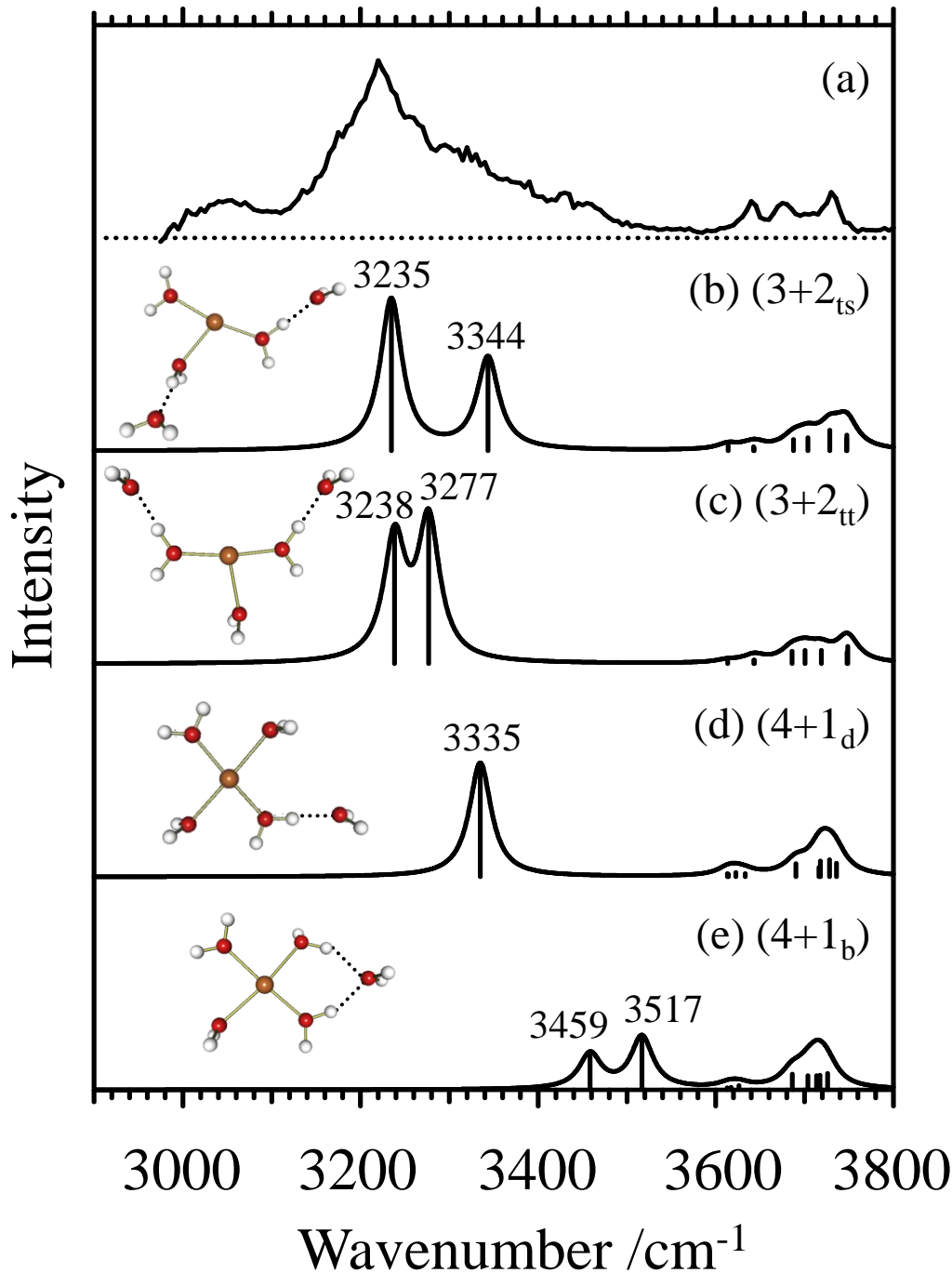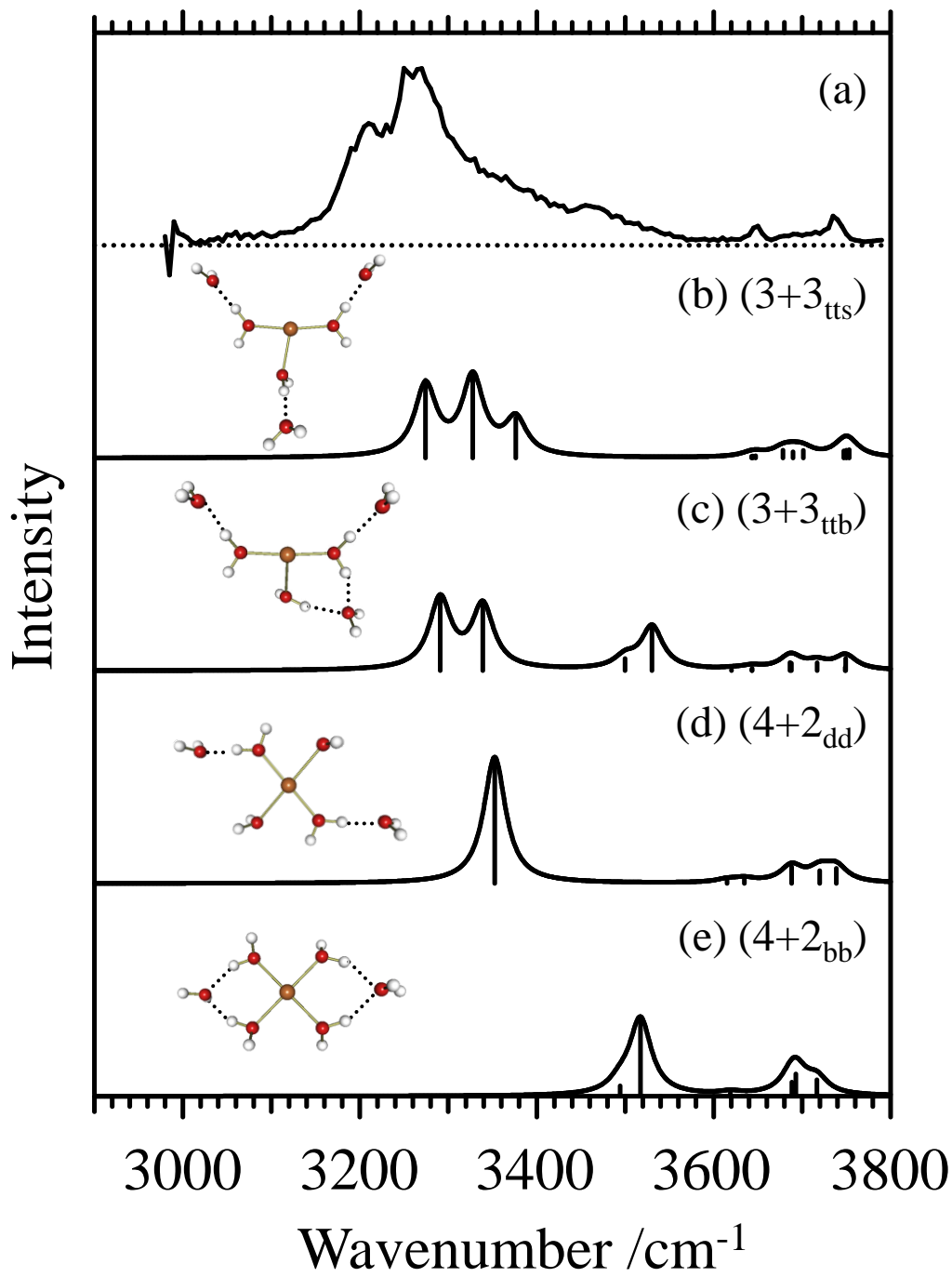(b) 2.02 2.24
(c) 2.15
(d) 1.94
(e)

Fig. 1 Furukawa et al.

Figure 2

Fig. 2 Furukawa et al.

Figure 3

Fig. 3 Furukawa et al.

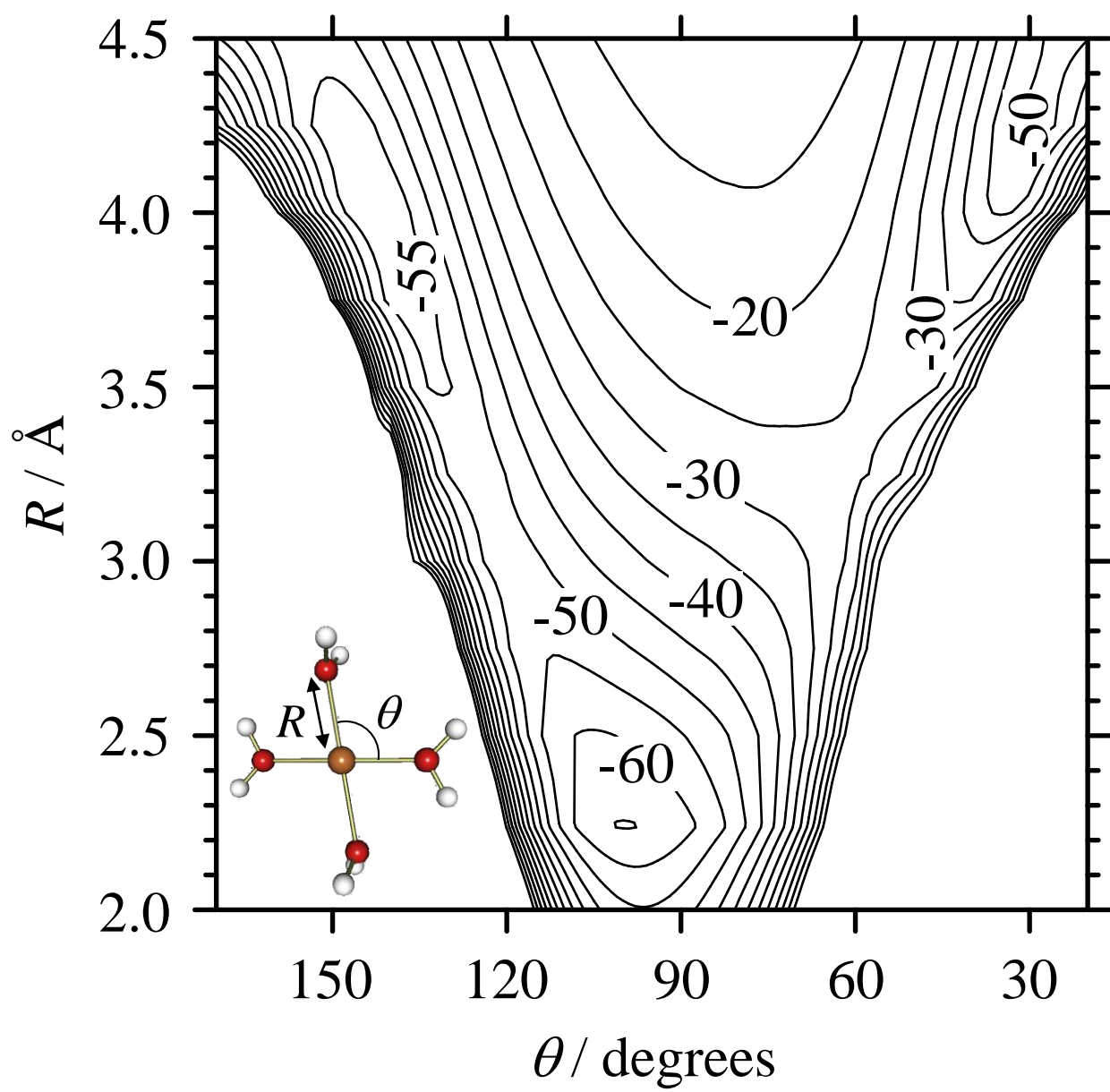Figure 4

(a)

(b) $(3+3_{tts})$

(c) $(3+3_{ttb})$

(d) $(4+2_{dd})$

(e) $(4+2_{bb})$

Intensity

3000 3200 3400 3600 3800

Wavenumber /cm^{-1}

Fig. 4 Furukawa et al.

Figure 5

Fig. 5 Furukawa et al.

Co⁺(H₂O)₃   **preference for H-bonding sites**